2012

A Nonlinear Model for Wind-Induced Oscillations of Trees

Lakshmi Narayanan Ramanujam
University of Massachusetts Amherst

A NONLINEAR MODEL FOR WIND-INDUCED OSCILLATIONS OF TREES

A thesis Presented

by

LAKSHMI NARAYANAN RAMANUJAM

Submitted to the Graduate School of the
University of Massachusetts Amherst in partial fulfillment
of the requirements for the degree of

MASTER OF SCIENCE IN MECHANICAL ENGINEERING

September 2012
MECHANICAL ENGINEERING

A NONLINEAR MODEL FOR WIND-INDUCED OSCILLATIONS OF TREES

A thesis Presented

by

LAKSHMI NARAYANAN RAMANUJAM

Approved as to style and content by:

_____

Yahya Modarres-Sadeghi, Chairperson

_____

Brian Kane, Member

_____

Jon McGowan, Member

_____

Donald L. Fisher
Professor and Department Head

DEDICATION

To everyone who has stood by me.

ACKNOWLEDGEMENTS

I would like to express my sincere and heartfelt gratitude to my advisor, Prof Yahya Modarres-Sadeghi, for his guidance and support during the course of my M.S. study at the University of Massachusetts Amherst. I would like to thank Prof Brian Kane and Prof Jon McGowan for agreeing to serve on the thesis committee and providing valuable feedback and suggestions. I would also like to thank Gary for his assistance and help when it was needed.

ABSTRACT

A NONLINEAR MODEL FOR WIND-INDUCED OSCILLATIONS OF TREES

09-01-2012

LAKSHMI NARAYANAN, B.TECH., SASTRA UNIVERSITY, INDIA

M.S.M.E., UNIVERSITY OF MASSACHUSETTS AMHERST

Directed by: Professor Yahya Modarres-Sadeghi

Ambient wind causes trees to oscillate. Wind-induced oscillations of trees constitute a fluid-structure interaction problem, which has been studied by many researchers from various points of view. However, there is yet a lot to be done. From an engineering point of view, the complex structure of trees, which are very different from man-made structures, as well as the highly nonlinear interaction between wind and tree, makes it a challenging task to predict the amplitude and frequency of the resulting oscillations. From a biological point of view, the influence of wind on photosynthesis as well as the growth and death of plants is crucial. A nonlinear model is derived for wind-induced oscillations of trees to investigate the effect of structural nonlinearities. It is shown that the structural nonlinearities in the system can result in a hardening behavior of the tree, indicating the importance of taking such nonlinearities into account. The influence of various system parameters such as tree's age, taper and slenderness ratio on the tree oscillations is studied using this nonlinear model.

TABLE OF CONTENTS

Page

LIST OF TABLES

Table Page

LIST OF FIGURES

Figure Page

CHAPTER 1

INTRODUCTION

1.1 Introduction

Wind-induced oscillations of trees have been studied for some time. Wind tends to influence the tree in several ways, from its growth to photosynthesis. Also, the potential risk of a tree subject to windthrow or a similar hazard presents a threat on various scales.

Trees evolve according to the wind loads that they experience and have a range of mechanisms to reduce the drag they experience in the wind. A combination of high wind loads and dead loads on the tree can ultimately cause the tree to fail. Tree failure, especially in urban areas can induce severe damage and even result in litigation (Mortimer and Kane, 2004). Understanding wind-induced oscillations can help in tree maintenance procedures to reduce the risk of such a failure. Procedures such as pruning can reduce the wind loading on a tree and thus reduce its susceptibility to failure (Smiley and Kane, 2006). In this thesis, the effect of the wind forces on the trees and the corresponding tree response will be studied.

1.2 Wind and tree

In general, wind has several direct or indirect effects on trees. Oscillations of trees and their effect on turbulence within the canopies of the structure are the direct results of wind blowing on trees. Windthrow is a direct result of gusts (Gardiner and Quine, 2000). Wind also affects photosynthetic processes of the leaves and the temperature of the leaves (Stokes et al., 2006). Through flutter of the outer leaves, wind also changes the

light entering the crown of the tree and thus influences photosynthesis again (Roden, 2003). The strains induced by wind can change the growth mechanism of the trees and their subsequent adaption to bear the self-weight of their trunks (Moulia et al., 2006). These biological influences have made it important to understand the effects of wind on trees.

Basically, trees are upright, flexible structures that have the ability to bend over in wind. For large trees especially, the diameter of the tree scales to its length by the power 1.5 (McMahon, 1973), which means that taller trees will have trunks with larger diameter. Younger trees will have more "flexibility" to bend over in wind and thus reduce the drag acting on them, while older trees will be less able to do so, and will be at a higher risk of windthrow and uprooting (Ennos, 1999). Hence, reconfiguration of trees to wind is quite an elegant way of solving the problem of reducing the drag on themselves and be less susceptible to wind forces that can damage them. They evolve and adapt to the environment in which the wind forces act on them in various ways, which include the "tapering of trunks and branches, streamlining their crown in high winds, thickening the sections under high stress to develop more strength, shedding leaves to reduce wind exposure and energy dissipation through high material damping and aerodynamic damping" (Haritos and James, 2009).

1.3 Tree structures and their response to wind

For a complete analysis of a tree structure, it is necessary to understand the dynamic loads acting on the tree, the magnitude of such forces and their frequency. A tree, typical of any species, consists of a trunk, branches, smaller branches and leaves or needles, which depend on the species of the tree. The strength i.e. Young's modulus, of such a

structure is complex and it can be understood by evaluating the size and the strength of each structural part in the tree. The trunk is normally the strongest of the lot, though its strength varies across its length due to its taper. The strength of the material in the tree also varies in different parts of the tree depending on the size and shape of the member. The strength of a younger tree is generally lower than that of an older one indicating the greater flexibility of the younger tree with respect to the older tree (James, 2003).

There are generally two types of loading on a tree: the static and the dynamic loads. The static loads consist of the weight of the branches and foliage besides the self-weight of the trunk, while the dynamic loads are due to the wind forces acting on the tree. The larger of the two forces are the dynamic forces on the tree. Owing to the fact that wind forces are neither constant nor periodic, it can produce a complex motion of the tree and its branches. Wind forces can cause an overturning moment on the base of the tree and if the stress induced by the force is greater than the bending stress of the trunk, it can result in a windsnap or a windthrow. Figure 1 illustrates the different types of failure of trees due to wind.

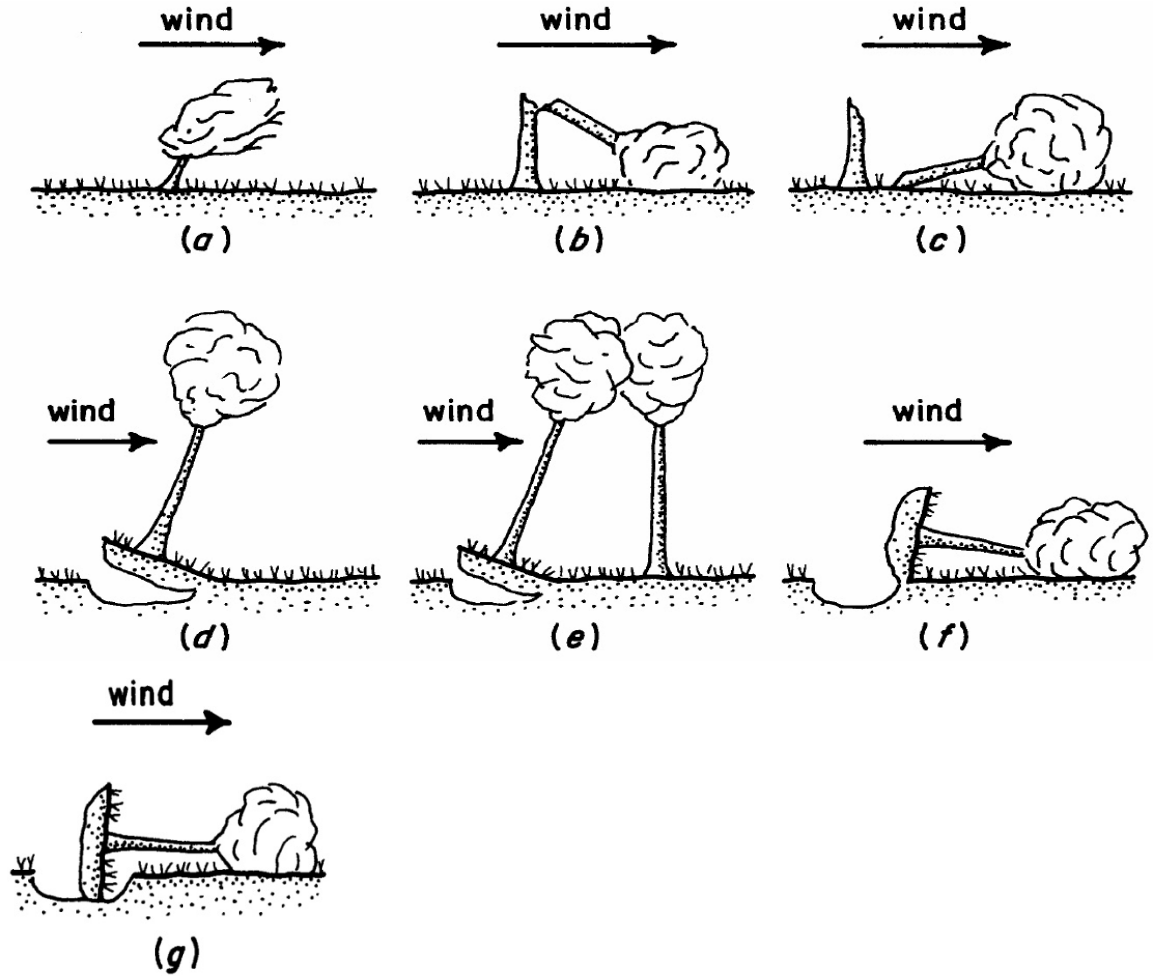

Figure 1: Different types of wind-damage and related ground features: (a) Windprune, (b, c) Windsnap, (d,e) Windtilt, (f,g) Windthrow (Allen, 1992).

1.4 Models for dynamic analysis of trees

A tree can be assumed as a cantilevered tapered beam with an end mass to represent the crown of the tree. The simplest model can assume a linear Euler-Bernoulli beam equation, with an external force due to wind:

$$\frac{\partial^2}{\partial x^2}(EI\frac{\partial^2 y}{\partial x^2}) + (\rho A + \rho_C A_C)\frac{\partial^2 y}{\partial t^2} = f \ , \tag{1}$$

where E is the Young's modulus of the spruce tree, I is the second moment of area of the cross-section of the trunk, A is the frontal area exposed to wind, ρ is the density of the

tree, ρ_c is the density of crown, A_c is the area of the crown and f is the force due to wind on the beam per unit length.

Wood, as a biological material has "anisotropic properties, is a composite material and is heterogeneous" (Spatz, 2000). Sections of a tree under stress stiffen over a long period of time while the tree itself is flexible to reduce the load. Therefore, it is "not always justified to use the simplifications of small deflections and linear responses" (Spatz, 2000).

In what follows, a summary of the major models used to predict wind-induced oscillations of trees is given.

1.5.1 Papesch model

Papesch (1974) developed a windthrow model to predict the oscillatory motion of individual plants. He assumed that the tree was a cantilevered beam acted upon by a component of turbulence from the wind with the same frequency as the natural frequency of the tree:

$$v = A_\omega \omega \cos \omega t , \tag{2}$$

where v is the velocity of the wind, ω is the frequency of the wind, A_ω is the amplitude of the wind gusts.

The drag on the tree is assumed to be proportional to velocity, v^2 and the damping ratio is a value that combined the aerodynamic damping, the damping from the branches and the damping from the root and soil – obviously a simplifying assumption. The stem is assumed to have a weight distribution identical to a conical tapered structure with uniform density.

The amplitude of tree vibration is calculated based on the assumption that the energy input from the wind was equal to the energy dissipated in the tree. The static deflection is calculated using the mean wind speed acting on the tree. The total amplitude of the tree oscillation at the top is found to be

$$A_T = \frac{\pi}{120} c_p c_d \rho \bar{v}^2 AH \frac{\theta^0}{R} + \frac{A_w}{0.625 + \frac{1.891 \xi \omega W}{\rho c_d \bar{v} A g}}, \quad (3)$$

where C_p is the center of pressure of the tree, C_d is the drag coefficient, ρ is the density of air, $\bar{v}$ is the mean velocity, A is the area of the crown, H is the height of the tree, R is the load acting on the tree, θ^0 is the angular deflection for a given load, R, A_ω is the amplitude of the wind component, ξ is the damping ratio of the tree and W is the weight of the stem and branches.

Using this model, Papesch predicts the velocity at which windthrow would occur. However, the model is basic in nature with rough estimation of tree parameters and does not take the crown into account as a separate mass. Moreover, the drag coefficient is assumed to be a constant (0.3) for various trees.

1.5.2 Gardiner model

A mathematical model was developed by Gardiner (1992) to predict the static and the dynamic responses of a tree in wind. Experiments were also performed to look at the mechanical behavior of the trees. In this model, the tree is assumed to be a damped harmonic oscillator. This is done by assuming the tree to be a beam with an end mass for the crown while neglecting the mass of the stem. The equation of motion for this tree is given by

$$m_e \frac{\partial^2 y}{\partial t^2} + c \frac{\partial y}{\partial t} + ky = F_o e^{i\omega t} \,, \tag{4}$$

where m_e is the equivalent mass of the tree, c is the damping coefficient, k is the spring constant and F_o is the amplitude of the wind force.

The physical characteristics of 10 Sitka spruce trees were estimated the resonant frequency of a 'standard' tree was estimated using all these values. This resonant frequency is given by

$$\omega = (\frac{385}{83} - 0.0023\omega^2)^{1/2} \,. \tag{5}$$

Using this relation, the resonant frequency is calculated and is found to be close to the natural frequency determined by pulling tests.

In this model, the drag force acting on the tree is assumed to have a mean and a fluctuating component. A power spectrum of the wind load is given by

$$P_F(\omega) = \rho_L^2 C_D^2 A^2 \overline{u}^2 P_u(\omega)(H_a(\omega))^2 \,, \tag{6}$$

where ρ_L is the air density, C_D is the drag coefficient , A is the projection area of the tree, $\overline{u}$ is the mean wind speed, $P_u(\omega)$ is the power spectrum of the horizontal wind speed and $H_a(\omega)$ is the aerodynamic transfer function. A power spectrum of the tree displacement is found by

$$P_d(\omega) = \frac{\rho_L^2 C_D^2 A^2 \overline{u}^2 P_u(\omega)}{m^2 \omega_h^4 ((1-(\omega/\omega_h)^2)^2 + (2\tau\omega/\omega_h)^2)} \,, \tag{7}$$

where ω_h is the frequency of undamped oscillations and τ is the damping ratio.

Then the tree response is modeled and compared with measured values in the field. The comparison between the theoretical and measured displacements for one Sitka spruce tree for which the physical characteristics were estimated is shown in Figure 4.

The normalized power spectrum, $fS_{dd}/\overline{d'd'}$ is shown in Figure 4 against the forcing frequency.

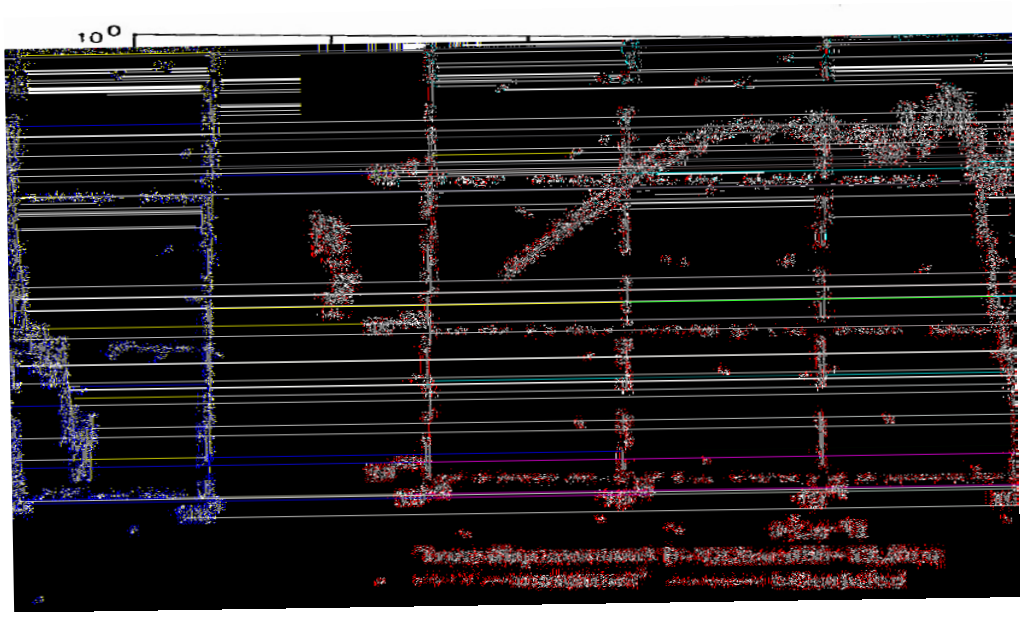

Figure 2: Actual and calculated normalized power spectra of tree displacement (Gardiner, 1992).

Even though this model predicts displacements close to the measured values for frequencies below the natural frequency of the tree, it does not predict accurate responses for frequencies higher than the resonant frequency. A damping ratio of 0.216 is used, increased by Gardiner from the original value of 0.054, to arrive at a good prediction of the displacement at frequencies close to natural frequency of the tree.

1.5.3 Kerzenmacher and Gardiner model

Kerzenmacher and Gardiner (1998) proposed a mathematical model to predict the response of a spruce tree in wind. Instead of considering the tree as a damped harmonic oscillator like Gardiner had done previously, the model tree was split into smaller segments, each with a mass, stiffness and damping parameter. These segments were joined together to set up the whole system that resulted in a set of coupled differential

equations. The tree for this model was split into 13 smaller segments. The set of equations could be written as

$$\underline{\underline{m}}\,\ddot{\underline{y}} + \underline{\underline{c}}\,\dot{\underline{y}} + \underline{\underline{k}}\,\underline{y} = 0\,, \tag{8}$$

where $\underline{\underline{m}}$, $\underline{\underline{c}}$ and $\underline{\underline{k}}$ are 13 × 13 matrices and $\underline{y}$ is the vector of displacement.

A transfer function was developed for the tree by solving the equations, which was further used to calculate the tree's response when subjected to wind forces. The calculated movements were then compared to the measured movements in the field. Figures 3 (a) and (b) illustrate the comparison between the calculated and the measured displacements at two different heights of the tree: at 8 m and 2 m, respectively.

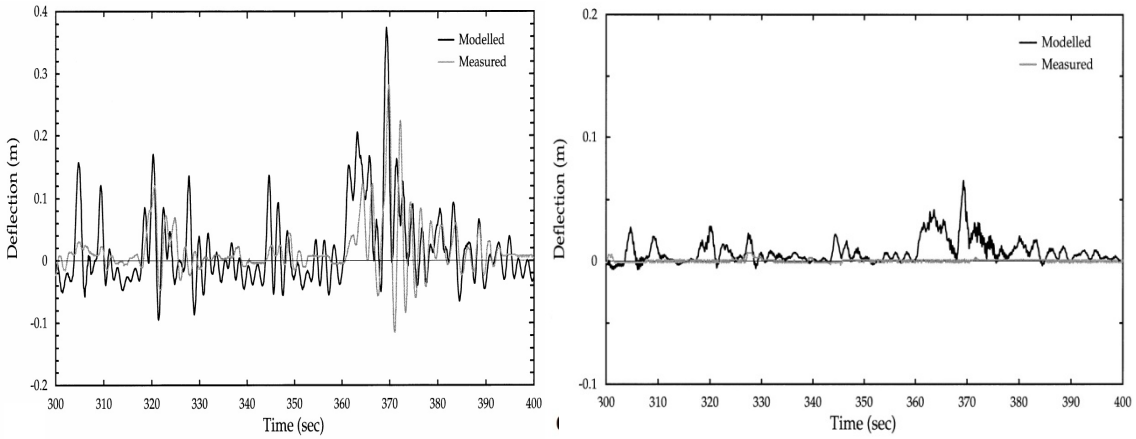

Figure 3: Modelled and measured displacements of the spruce tree at (a) 8 m, (b) 2 m (Kerzenmacher and Gardiner, 1998).

As seen in the two figures, this model predicts the deflections well at the top of the tree but fails to do so at lower heights of the tree at frequencies above the resonant frequency of the tree. This might have been due to lumping of the branches with the stem rather than treating them as individual cantilevers attached to the main cantilever representing the stem.

1.5.4 Peltola model

Peltola et al. (1999) developed a model to assess the risk of wind and snow to single trees and stands. The model, called HWIND, predicts the critical turning moment and the failure wind speed at which the trees will be uprooted or break. This was calculated for trees at forest margins. The turning moment on the tree is calculated by estimating the force on the stem and the crown. The force on the tree is assumed to be a combination of the wind force and the force due to gravity. The total mean wind-induced force on the tree is calculated by summing up the forces acting at each point along the stem and the crown:

$$F_1(z) = \frac{C_D \times \rho \times u(z)^2 \times A(z)^2}{2}\ , \tag{9}$$

where C_D is the drag coefficient, ρ is the density of air, $u(z)$ is the mean wind speed and $A(z)$ is the projected area of the tree against the wind at height z. The wind profile is assumed to be logarithmic near the edge of the forest.

The force from the bending of the tree due to gravity is obtained by summing up the forces on 1-m segments of the tree along the whole length. This force is

$$F_2(z) = M(z) \times g\ , \tag{10}$$

where $M(z)$ is the mass of the stem and the crown, g is the acceleration due to gravity.

The model is fed inputs on diameter, height, modulus of elasticity, stem density, crown width, crown height, drag coefficient, etc. If the total turning moment of the tree exceeds the support provided by root-soil plate, the tree is assumed to break. The tree is assumed to be uprooted if the bending moment is greater than the moment that could be withstood by the tree. Though the predicted values are in good agreement with tree-pulling experiments performed on Scots pine, Norway spruce and birch, the model was

found to be quite sensitive to the input parameters. Figure 7 shows the comparison between the predicted critical turning moment by HWIND and the experimental values performed on Scots pine shown by DBASE.

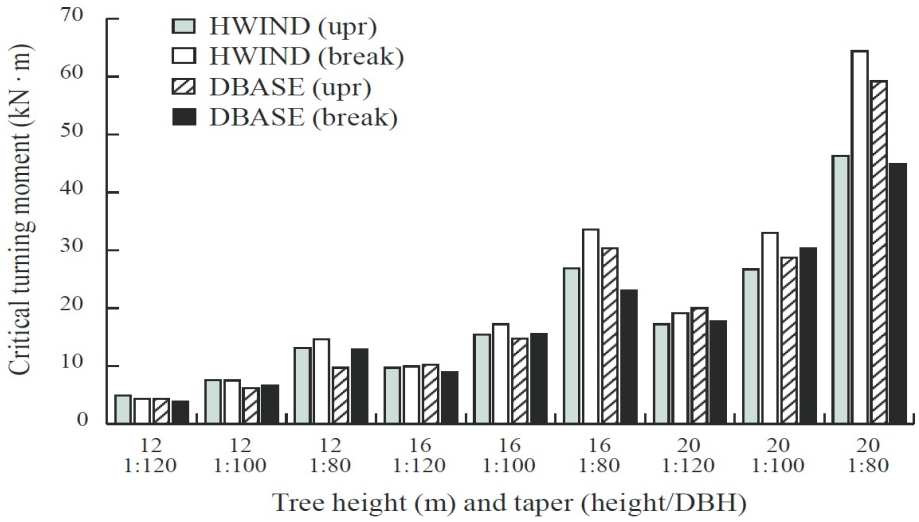

Figure 4: Prediction of HWIND model as compared to experimental values (Peltola et al., 1999).

1.5.5 Saunderson model

To predict the dynamic response of the Sitka spruce tree in high winds, a model was developed by Saunderson et al. (1999). The model assumes that the trunk of the tree can be represented by a vertical tapered cantilever and the crown by a cylindrical body at the top of this trunk. This model is used with favorable results for the spruce tree in predicting its failure wind speeds. The beam equation is

$$\frac{\partial^2}{\partial x^2}(EI\frac{\partial^2 y}{\partial x^2})+\rho A\frac{\partial^2 y}{\partial t^2}=f \ , \tag{11}$$

where y is the inline deflection of the tree, EI is the flexural rigidity of the tree, ρ is the density of the tree, A is the frontal area exposed to the wind and f is the drag force on the tree. The drag force on the tree is

$$f = \frac{1}{2}\rho_a A_E C_D u_r^2 , \tag{12}$$

where ρ_a is the density of air, A_E the frontal area, C_D the drag coefficient and u_r the relative velocity of the tree which in turn is given by (u-$\dot{y}$). The model assumes that the wind acts at the top of the crown, rather than along the length of the tree. The drag force is assumed to act on the crown only. The velocity of the wind can be assumed to have a mean and a fluctuating component where $u=u_m + u_f$, where u_m is the mean velocity and u_f is the fluctuating velocity. Consequently, equation 11 gives rise to two equations, one for the mean displacement and one for the fluctuating displacement. The equation for the mean displacement equation is

$$E I y_m'''' = \frac{1}{2}\rho_a A_E C_D u_m^2 , \tag{13}$$

and the equation for the fluctuating displacement equation is

$$E I y_f'''' + m \ddot{y}_f + \rho_a A_E C_D u_m \dot{y}_f = \rho_a A_E C_D u_m u_f , \tag{14}$$

In these equations, the taper of the trunk is taken into account as is the crown density of the tree. Transfer functions are used for comparing the tree displacement spectra from the model to those derived from the experimental data. Figure 8 shows the spectra for both theoretical and experimental deflections for two Sitka spruce trees, where *H(n)* is a dimensionless transfer function indicating the displacement of the tree. The model gives a good prediction of the natural frequency and matches the experimental data upto 0.7 Hz, but not for higher frequencies.

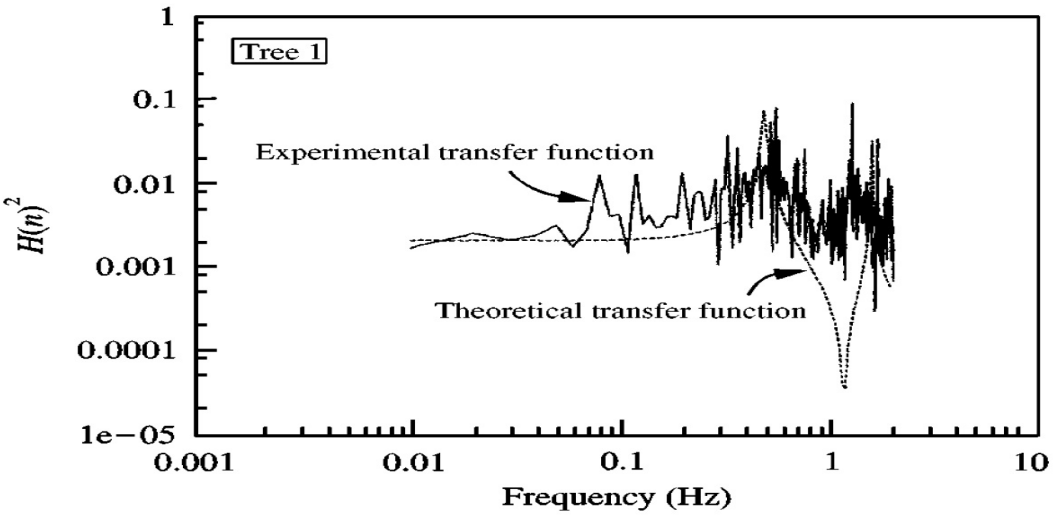

Figure 5: Calculated and observed displacement spectra for Sitka spruce (Saunderson et al., 1999).

All the models discussed above assume the structure to be linear. Also, the drag coefficient is assumed to be constant and does not change with tree's oscillations, which is not necessarily the case. Drag coefficient varies with the magnitude of tree's oscillations and also with the wind speed (Mayhead, 1973; Kane et al, 2008; Smiley and Kane, 2006). In this project, the structure will be modeled as a nonlinear Euler-Bernoulli beam equation and under the influence of the drag force.

CHAPTER 2

A NONLINEAR MODEL TO PREDICT THE OSCILLATION OF TREES IN WIND

A nonlinear model is developed to predict the oscillation of trees in wind. The tree is modeled as a nonlinear cantilevered Euler-Bernoulli beam subjected to fluctuating drag force. This model is used to investigate the importance of a nonlinear model for the structure in the resulting tree response.

2.1 The nonlinear model

The nonlinear model is obtained by assuming the structure to be a nonlinear Euler-Bernoulli beam, subjected to a fluctuating drag force:

$$\begin{aligned} &EI(x)y''''+(\rho+\rho_c(x))A(x)\ddot{y}+EI(x)\left[y'^2\,y''''+4y'\,y''\,y'''+y''^3\right]+\\ &EI'(x)[2y'''+y'^2\,y''''+4y'\,y''\,y'''+y''^3]+EI''(x)y''\,y'^2+\\ &y'\int_0^L(\rho+\rho_c(x))A(x)(\dot{y}'^2+y'\,\ddot{y}')ds-y''\int_s^l\int_0^s(\rho+\rho_c(x))A(x)(\dot{y}'^2+y'\,\ddot{y}')dsds=F \end{aligned} \quad , \tag{15}$$

where y is the inline deflection of the tree, ()' is the derivative with respect to x, ($\dot{}$) is the derivative with respect to time, $EI(x)$ is the flexural rigidity of the tree, ρ is the density of the wood, $\rho_c(x)$ is the density of the crown, $A(x)$ is the cross-sectional area and F is the drag force on the tree which can be written as

$$F=\frac{1}{2}\rho_a A_E C_D(U-\dot{y})^2\,, \tag{16}$$

where ρ_a is the density of air, $A_E(x)$ the frontal area, C_D the drag coefficient, $U(x)$ the wind speed and $\dot{y}$ is the velocity of the tree.

In this model, the tree's cross-sectional area A(x), its flexural rigidity EI(x) and flow profile can vary along the length of the tree. In dimensionless form, this equation reads as

$$\eta''''+\ddot{\eta}+\left[\eta'^{2}\eta''''+4\eta'\eta''\eta'''+\eta''^{3}\right]+$$
$$\hat{I}'(\xi)[2\eta'''+\eta'^{2}\eta''''+4\eta'\eta''\eta'''+\eta''^{3}]+\hat{I}''(\xi)\eta''\eta'^{2}+$$
$$\eta'\int_{0}^{1}(\dot{\eta}'^{2}+\eta'\ddot{\eta}')ds-\eta''\int_{\xi}^{1}\int_{0}^{\xi}(\dot{\eta}'^{2}+\eta'\ddot{\eta}')d\xi d\xi=\alpha(\xi)+\beta(\xi)\dot{\eta}^{2}-\gamma(\xi)\dot{\eta}$$

(17)

where the dimensionless parameters used are

$$\eta = y/l \tag{18}$$

$$\xi = x/l \tag{19}$$

$$\tau=\frac{t}{l^{2}}\sqrt{\frac{EI}{(\rho+\rho_{c})A}} \tag{20}$$

$$\alpha=\frac{\rho_{a}A_{E}C_{D}l^{3}U(x)^{2}}{2EI(x)} \tag{21}$$

$$\beta=\frac{\rho_{a}A_{E}(x)C_{D}l}{2(\rho+\rho_{c})A} \tag{22}$$

$$\gamma=\frac{\rho_{a}A_{E}(x)C_{D}l^{3}U(x)}{2\sqrt{EI(x)(\rho+\rho_{c})A(x)}} \tag{23}$$

2.2 Method of solution

The equation of motion is a nonlinear partial differential equation, which is discretized by Galerkin's method using the eigenmodes of a cantilevered beam as the base functions:

$$\eta(\xi,\tau)=\sum_{n=1}^{N}\varphi_{n}(\xi)q_{n}(\tau), \tag{24}$$

where φ_n are the eigenfunctions of a cantilevered beam and $q_n(t)$ are the generalized coordinates of the discretized system. Six modes are used in discretization.

The ordinary differential equations obtained after discretization are then solved using Houbolt's method, in which the first and second order derivatives of the generalized coordinates are approximated by

$$\ddot{x}_{j,n+1} = \frac{\left[2x_{j,n+1} - 5x_{j,n} + 4x_{j,n-1} - x_{j,n-2}\right]}{(\Delta t)^2} \tag{25}$$

and

$$\dot{x}_{j,n+1} = \frac{\left[11x_{j,n+1} - 18x_{j,n} + 9x_{j,n-1} - 2x_{j,n-2}\right]}{(6\Delta t)^2}, \tag{26}$$

where $x_{j,n} = x_j(n\Delta t)$ and Δt is the time step.

The Newton-Raphson method is used to find the solution of the resulting nonlinear matrix equation in each step (Semler et al., 1996). In what follows, this model is used to study the influence of structural nonlinearity on wind-induced oscillations of trees.

CHAPTER 3

RESULTS – TREE RESPONSE

3.1 Response of a tree with constant diameter

As a first step, a tree with a constant diameter is considered. A model with a linear structure and a nonlinear structure are considered. The parameters are given in Table 3.

Table 1: Parameter specifications from the experiment used for the model.

Parameters	Values
Length (m)	16.5
Density of wood (kg/m^3)	428.63
Modulus of elasticity (N/m^2)	1.2×10^9
Average diameter (m)	0.244
Base diameter (m)	0.533
Drag coefficient, C_D	0.4
Density of air (kg/m^3)	1
U (m/s)	5

Figure 6 shows the dimensionless amplitude of the tree's tip oscillations versus the dimensionless wind frequency. The circles correspond to the results with the linear structure (found by solving equation (15) and keeping only the first two terms in the left hand side and neglecting all other terms). These results are obtained by solving the nonlinear equation where the nonlinearities come from the flow force only and they show that, as expected, the tree has the largest response, when the frequency of the fluctuating drag force is equal to the natural frequency of the structure (a dimensionless frequency of 1). At other frequencies, the response has smaller amplitudes and for external frequencies far enough from the natural frequency, the response is very small. When the structural nonlinearities are considered (i.e., when all the terms on the left hand side of equation

(15) are kept in the solution) the response (pluses) bends to the right. These results show that the nonlinear effect (hardening) is due to the structural nonlinearities, as the effect disappears when the structural nonlinearity is removed from the model. The hardening effect suggests that for any frequency in the range of dimensionless frequencies between 1.14 and 1.2 for this set of parameters, the tree can have two stable solutions. This implies that in this range of frequencies, the tree can oscillate with either a low amplitude of around 0.05 times its length (the lower branch in the plot) or a large amplitude of around 0.15 of its length (the upper branch in the plot), depending on the initial conditions(the initial disturbance which triggers the oscillations). As an example, if the wind speed has a frequency of 1.2 Hz, then the tree's maximum amplitude of oscillation could be either (0.04)(16.5) = 0.66 m or (0.15)(16.5) = 2.475 m. The model with the linear structure does not predict the large amplitude oscillations in the high-frequency region. The amplitude of oscillation predicted by this model at $f/f_n = 1$ reduces by approximately 75 percent when structural nonlinearities are considered. This means that due to the structural nonlinearities, the maximum amplitude shifts from $f/f_n = 1$ to a larger frequency.

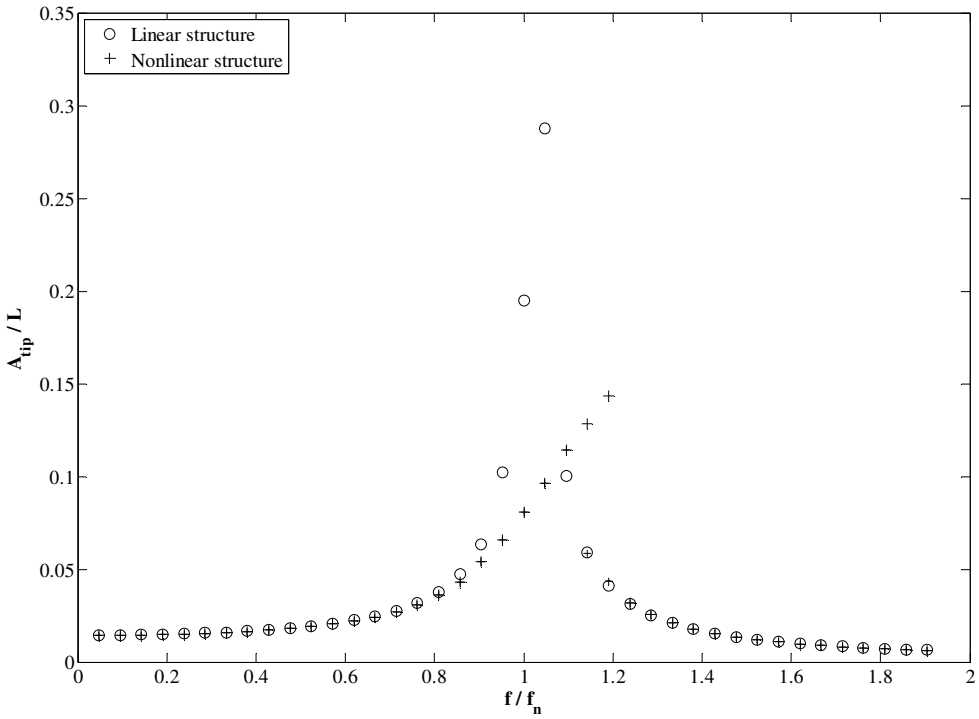

Figure 6: Nondimensional amplitude of oscillation versus frequency of wind speed for a tree with force along whole length, the linear and nonlinear structure coupled with flow.

3.2 The influence of various wind profiles

Trees can be subjected to wind velocities with various profiles. To investigate the influence of these profiles on the hardening effect discussed in previous section, four different flow profiles are considered. The first two flow profiles follow a power law to define the wind shear (Ray et al., 2006):

$$\frac{U_x}{U_{\max}} = \left(\frac{x}{l}\right)^{\alpha}, \tag{27}$$

where the velocities, U_x and U_{max} are the velocities at x and l. The power law exponent α is chosen according to the terrain. For the first flow profile, a power law exponent of 0.24 is chosen, which is expected in a place with trees and small buildings around. For

the second flow profile, a power law of 0.13 is chosen. The other two profiles are uniform flow and linearly sheared flow. The four different profiles of wind are shown in Figure 7.

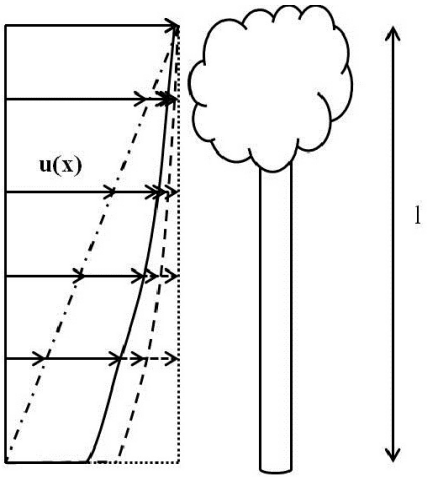

Figure 7: Wind shear profile with linear shear (dashed-dotted line), α ,as 0.13 (dashed line), 0.24 (continuous line) and uniform flow (dotted line).

Figure 8 shows the response for all the wind profiles for a maximum flow velocity of 5 m/s. As seen in the figure, the hardening nonlinearity exists for all wind profiles.

The maximum amplitudes increase slightly for the uniform flow and the shear parameter of 0.13, compared to the other two profiles as the shear exponent, α decreases. As α decreases, the energy input into the structure increases resulting in higher amplitude and a more pronounced hardening effect. The presence of hardening effect for all the flow profiles considered indicates that structural nonlinearities are playing a role irrespective of the flow.

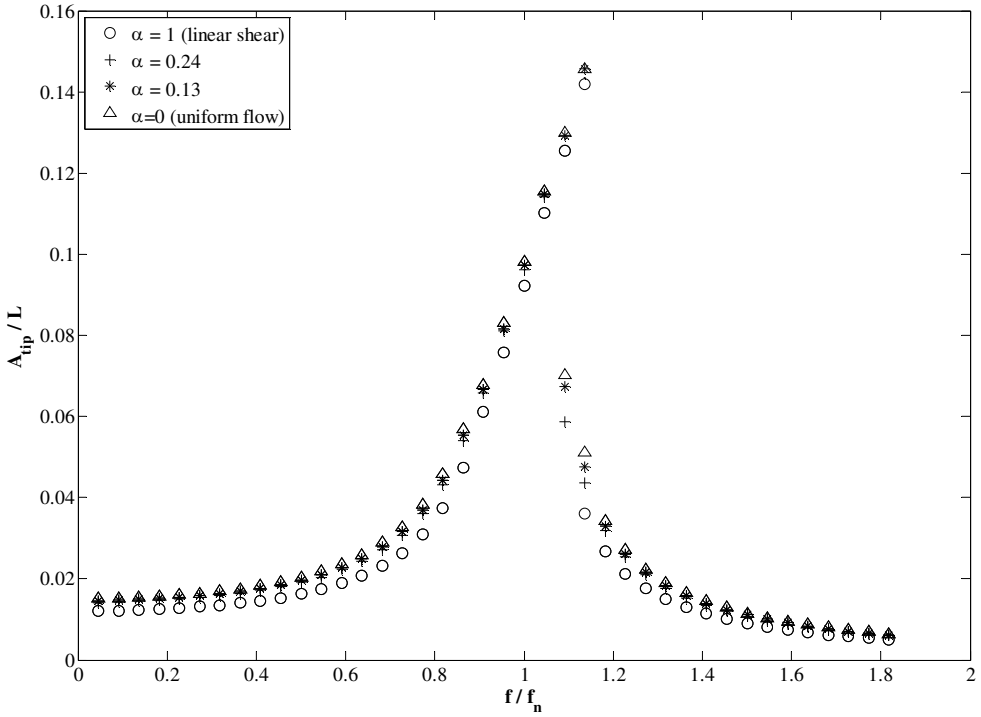

Figure 8: Nonlinear model with as 0, 0.13, 0.24 and 1with a maximum velocity of 5 m/s.

Figure 9 shows the maximum nondimensional amplitude for α=0-1 and for a maximum velocity of 5 m/s. As the shear parameter increases, the nondimensional amplitude for the system decreases.

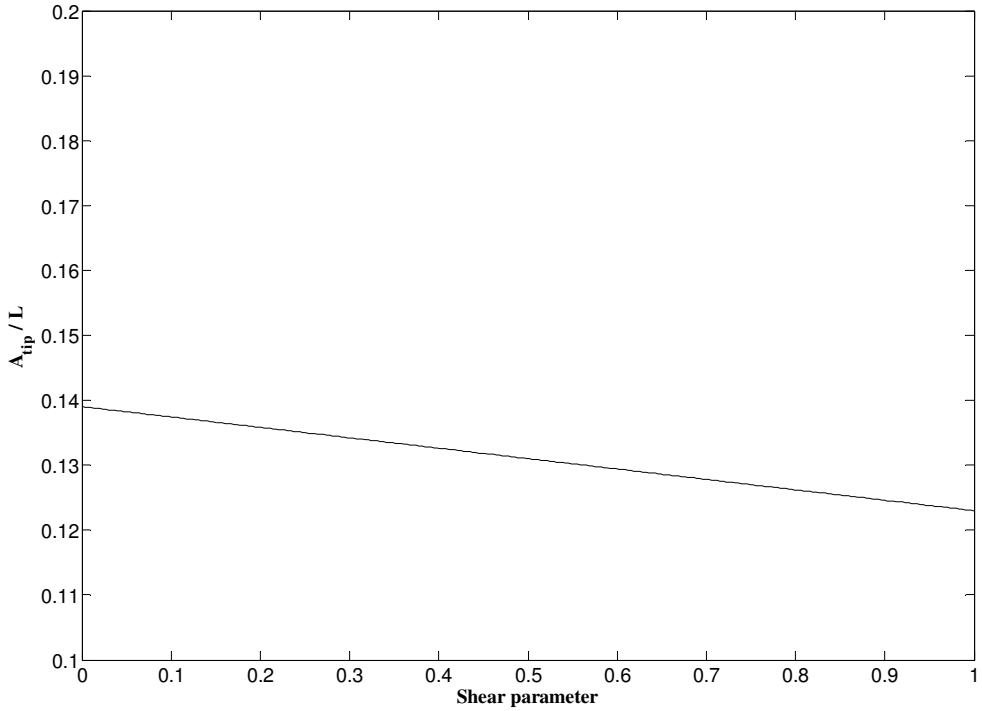

Figure 9: Dimensionless maximum amplitude for a maximum velocity of 5 m/s and different shear parameters.

Figure 10 shows the tree response for the power law exponent of 0.24 and different maximum velocities. For wind velocities as low as 2 m/s, the structure shows a hardening nonlinearity in its response and the hardening effects increase as the maximum flow velocity increases. Overall, it is seen that changing the flow profile does not affect the results dramatically. The maximum flow is a more critical value in changing the resulting maximum speed. In any case, the hardening effect is observed.

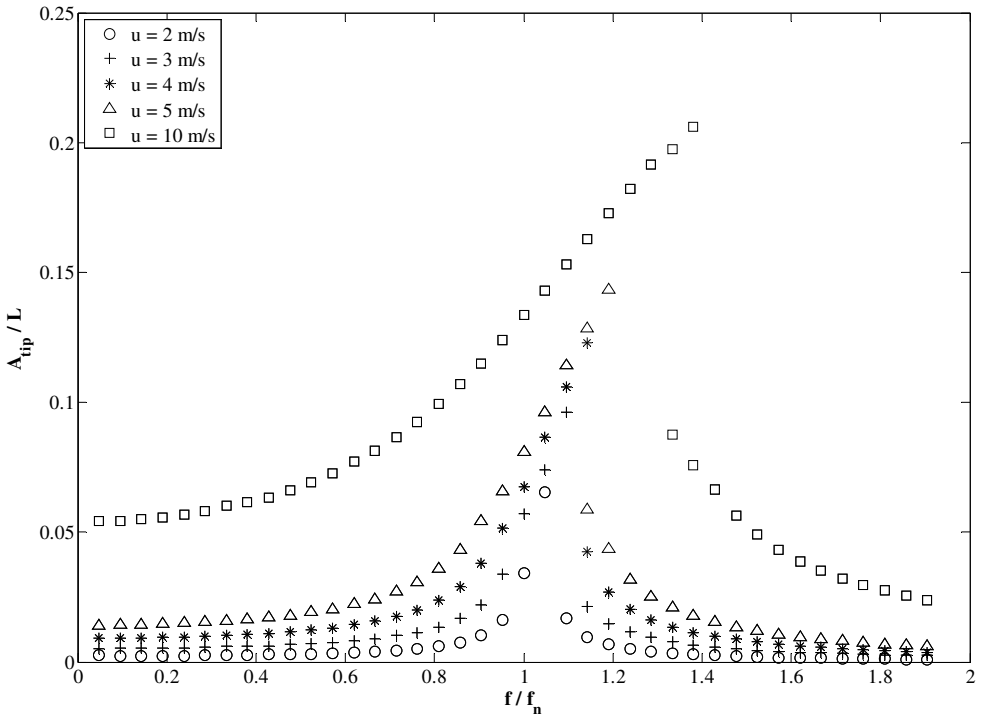

Figure 10: Nonlinear model with wind shear and various maximum velocities.

3.3 The influence of wind-velocity dependent drag coefficient

It is shown that the drag coefficient varies with the wind speed (Mayhead, 1973; Kane et. al, 2008; Kane and Smiley, 2006). Mayhead used experimental data of various species to calculate regression lines for the drag coefficient as a function of wind speed as

$$C_D = C + m_1 u + m_2 u^2, \tag{28}$$

where m_1 and m_2 are regression coefficients that have values depending on the tree species (Table 2).

Table 2: Measured drag and regression coefficients for different trees (Mayhead, 1973).

Tree	C_D	C	m_1	m_2
Sitka Spruce	0.35	0.86	-0.0095	-0.0036
Corsican Pine	0.32	1.135	0.0045	0.0015
Lodgepole Pine	0.2	0.63	0.002	-0.0009
Scots Pine	0.29	0.9117	-0.051	0.0012

Mayhead also found that there was a variation in the drag coefficients within a tree species. Experiments conducted on other species (e.g. Kane et al., 2008, Kane and Smiley, 2006) showed a similar trend in variation of the drag coefficient with wind speed. Figure 11 shows the response of the system for a constant drag coefficient of 0.29 and a variable drag coefficient. The maximum wind speed is 5 m/s and the power law exponent is 0.24. To include the change in drag coefficient with respect to velocity, the regression coefficients, i.e. C, m_1 and m_2, were chosen from Mayhead's experiments on the Scots Pine (Mayhead, 1973). Due to a higher value for the drag coefficient for the same velocity, the tree experiences a larger maximum amplitude, for a varying drag coefficient. For both cases, the nonlinearities are apparent in the response.

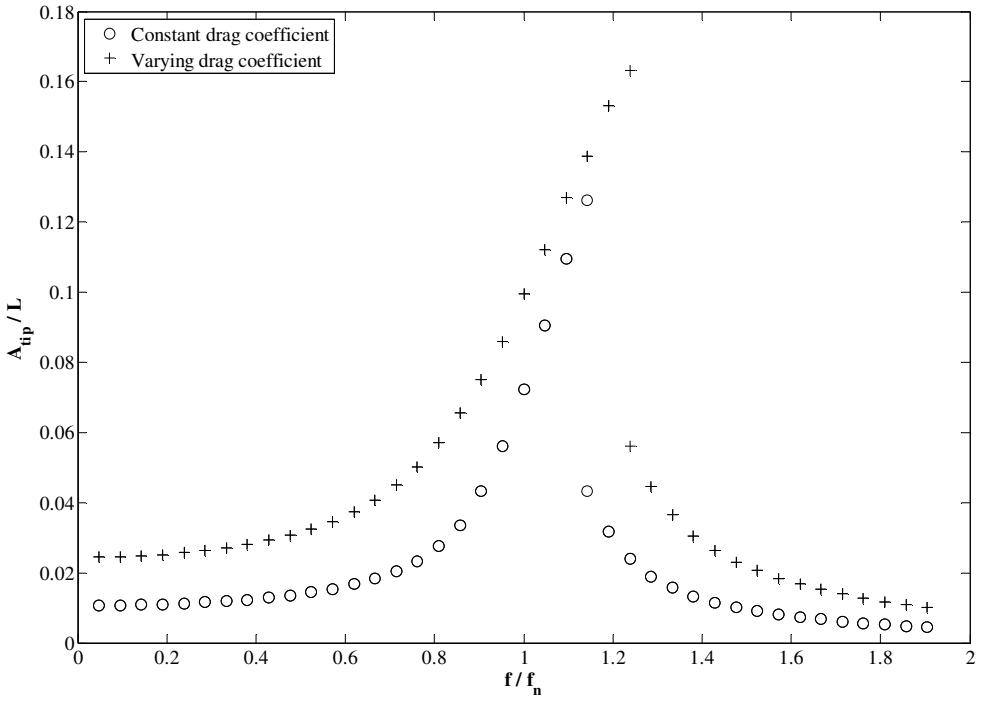

Figure 11: Nonlinear model with a constant and varying drag coefficient and a maximum velocity of 5 m/s.

3.4 The influence of trunk's taper

In reality, a tree's trunk tapers as a function of height. To accommodate for the effect of the taper on the response of the tree, a taper parameter is used as

$$\lambda = (D - d) / l$$

where D and d are the diameters at the bottom and top of the trunk respectively; and l is the length of the tree. Thus, a taper parameter of 0 corresponds to a tree with constant diameter. Figure 12 shows the response of the tree oscillation for different taper parameters and for a maximum velocity of 5 m/s and a shear parameter of 0.24. The maximum amplitude of the tree reduces as the taper parameter increases, which is mainly due to the reduction of frontal area due to taper. This is in agreement with what has

already been observed for tall buildings by Kim and You (2004). Figure 13 shows the reduction in maximum amplitude of the tree.

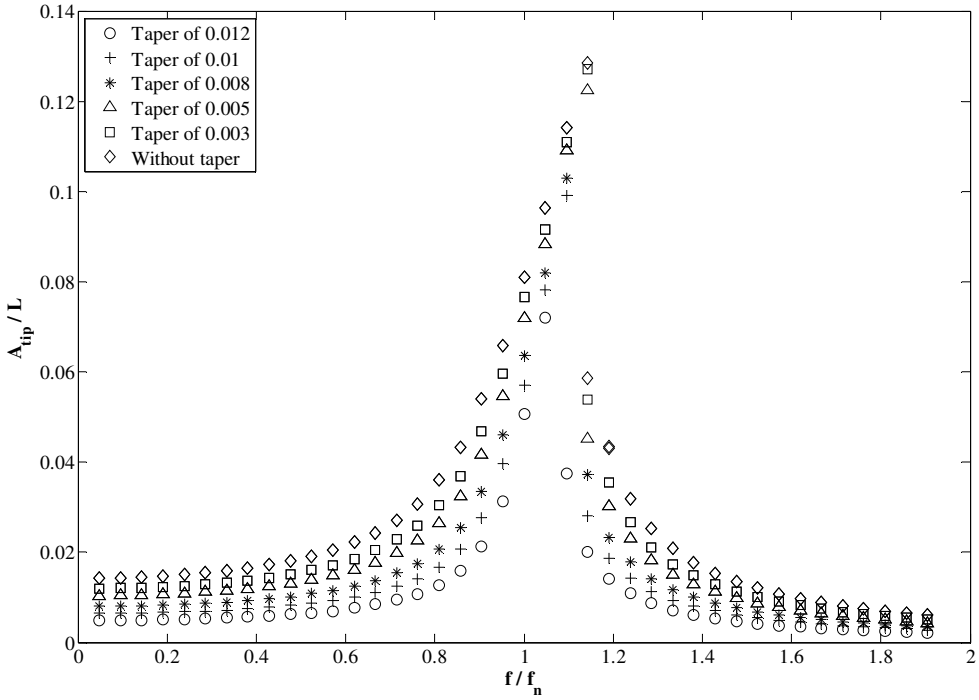

Figure 12: Nonlinear model with a maximum velocity of 5 m/s and different taper parameters.

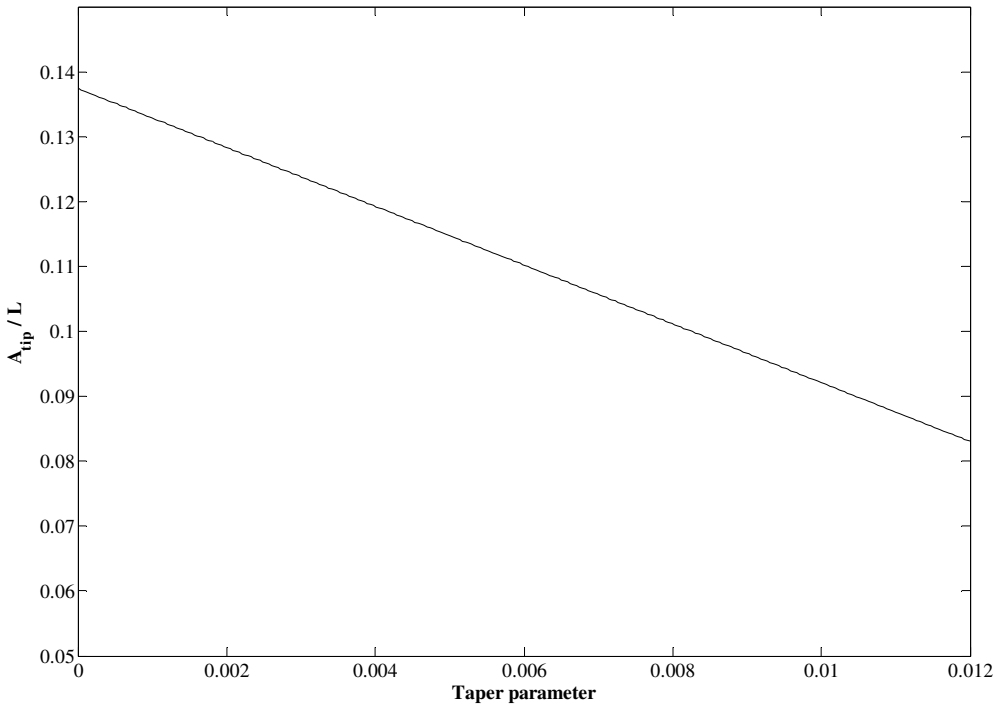

Figure 13: Nonlinear model with maximum amplitude and different taper ratios.

3.5 Slenderness ratios

The slenderness ratio of a structure is given by the ratio of its height to its diameter (L/D). Figure 14 shows the tree response for various slenderness ratios with a power law exponent of 0.24, a maximum wind speed of 5 m/s and a constant drag coefficient of 0.4. The original slenderness ratio of the tree was 67.62.

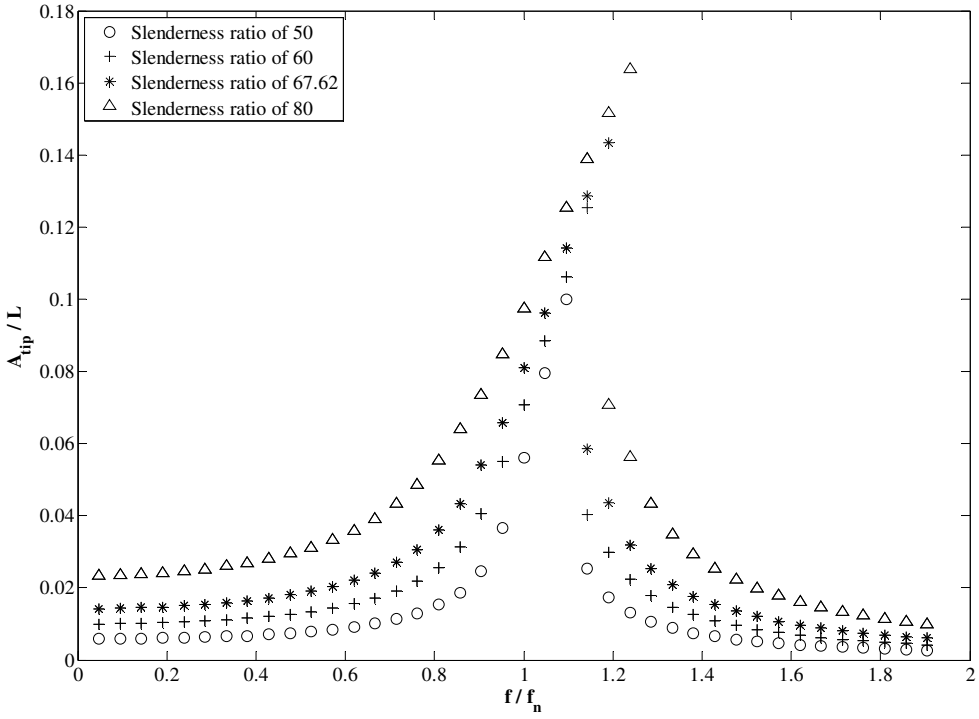

Figure 14: Nonlinear model with different slenderness ratios and a maximum velocity of 5 m/s.

The hardening effects are observed for all slenderness ratios. Apart from the increasing amplitudes, the hardening effects are more profound with increasing slenderness ratio. This is expected as a larger aspect ratio results in a larger flexibility of the tree, and therefore a more significant nonlinear behavior of the structure. Figure 15 represents the maximum amplitude for various slenderness ratios. As the slenderness ratio increases, the maximum amplitude increases linearly.

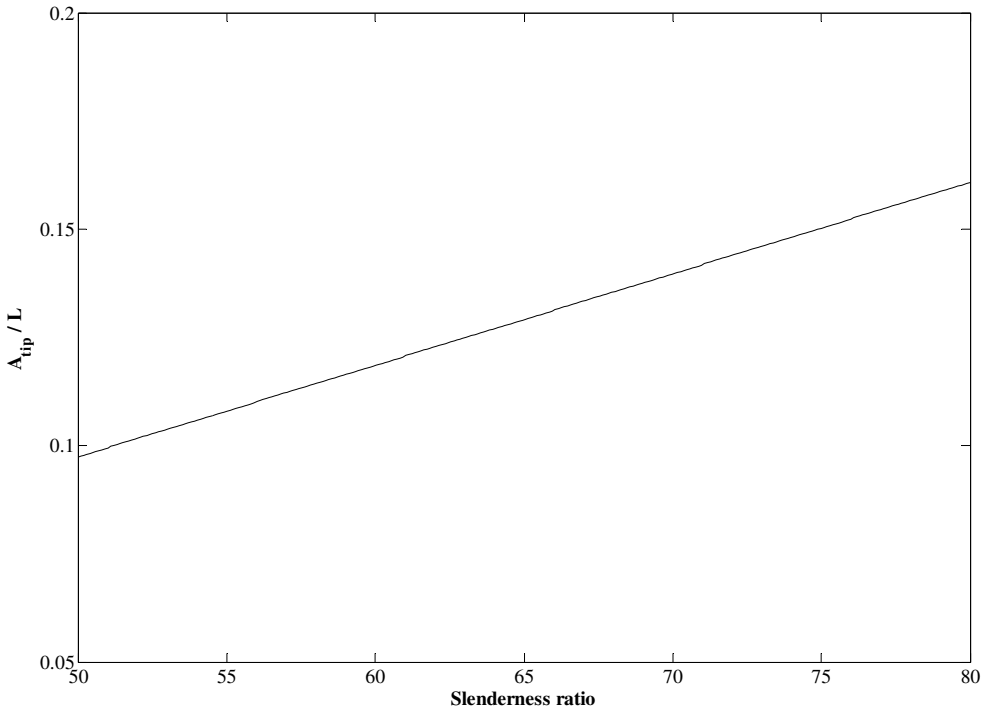

Figure 15: The maximum amplitude of oscillations with various slenderness ratios. The maximum velocity is 5 m/s, the drag coefficient 0.4 and the power law exponent 0.24.

3.6 A discussion on the dynamical response of the younger trees versus the older trees

To look at how younger trees behaved in comparison to an older tree, the material properties are chosen for a younger tree. The average Red Pine grows 0.3 m every year. The height of the Red Pine for a younger tree was thus chosen with relevance to its age. The diameter was calculated by keeping the slenderness ratio constant as 67.62. Table 3 shows the parameters used for the younger trees.

Table 3: Properties of trees with age.

Age	E (*10^9 N/m^2)	*Density (kg/m^3)*	*Height (m)*
5	0.6	248	1.5
10	0.6	268	3
15	0.75	288	4.5
20	0.75	308	6
25	0.9	328	7.5
30	0.975	348	9

Deresse (1998) investigated the growth properties of Red Pine. The simulations were performed for 10-, 20- and 30-year-old Red Pines. The Red Pine used for previous calculations was estimated to be 40-60 years old. Figure 16 shows the response of younger trees with a shear parameter of 0.24 and a maximum velocity of 5 m/s.

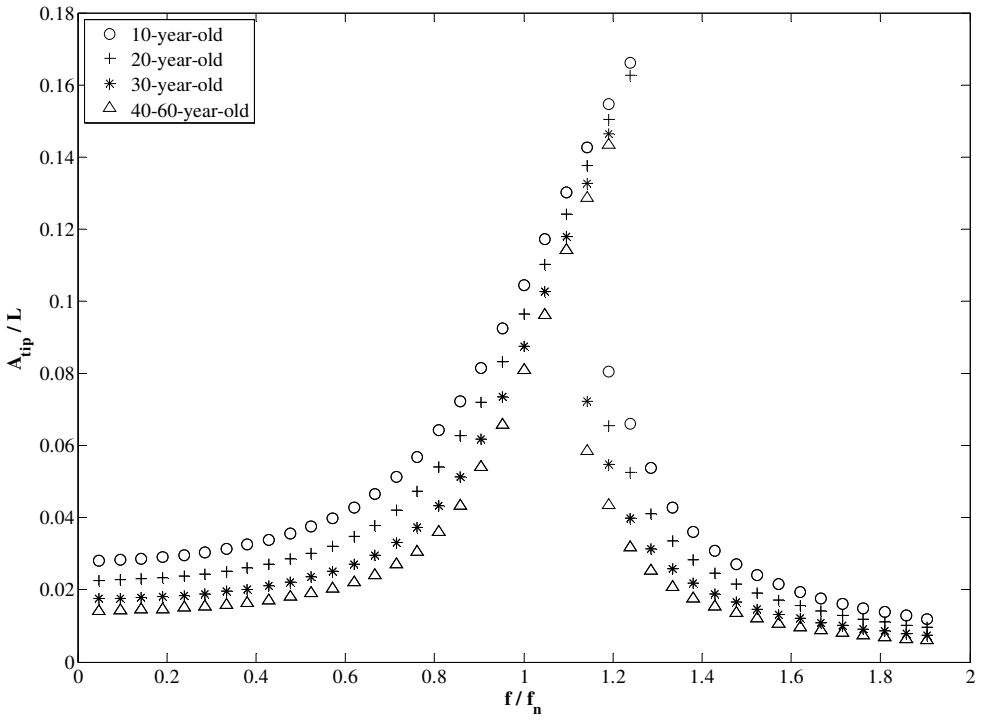

Figure 16: **Nonlinear model with a maximum velocity of 5 m/s for comparison with younger trees.**

The hardening effects for the younger trees are more pronounced than the older tree. The higher amplitudes for the younger trees may be due to their lower flexural rigidity. The stiffness in younger trees is lower, making them more flexible to bend over in wind. This, in turn, results in higher amplitudes. In this case, it also lends to more nonlinearity for the younger trees. Figure 17 shows the trend of the maximum amplitude with a maximum velocity of 5 m/s. It can be observed that the amplitude decreases slightly with age. This might be due to the stiffening of the trunk with age that leads to a smaller deflection when it is older.

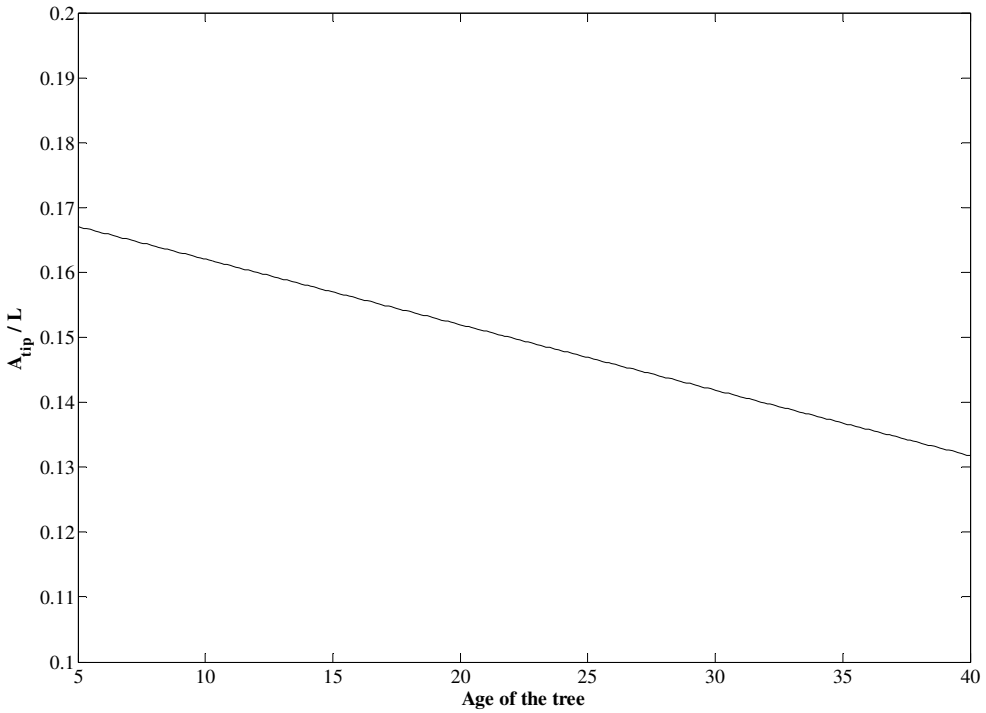

Figure 17: The maximum amplitude of oscillations for trees of different ages. The maximum velocity is 5 m/s.

3.7 The influence of variable mass per unit length and flexural rigidity along the length

Spatz et al. (2007) investigated the branches for their properties in a Douglas fir, measuring the change in flexural rigidity, mass per unit length and the cross-sectional area along their lengths. This variation in the properties is included in the model to look at the response of a typical branch. Figure 18 shows the trend of the amplitude of the branch for a uniform flow of 5 m/s. The nonlinear effects are evident in the plot, with the branch showing its maximum amplitude at a frequency above its natural frequency.

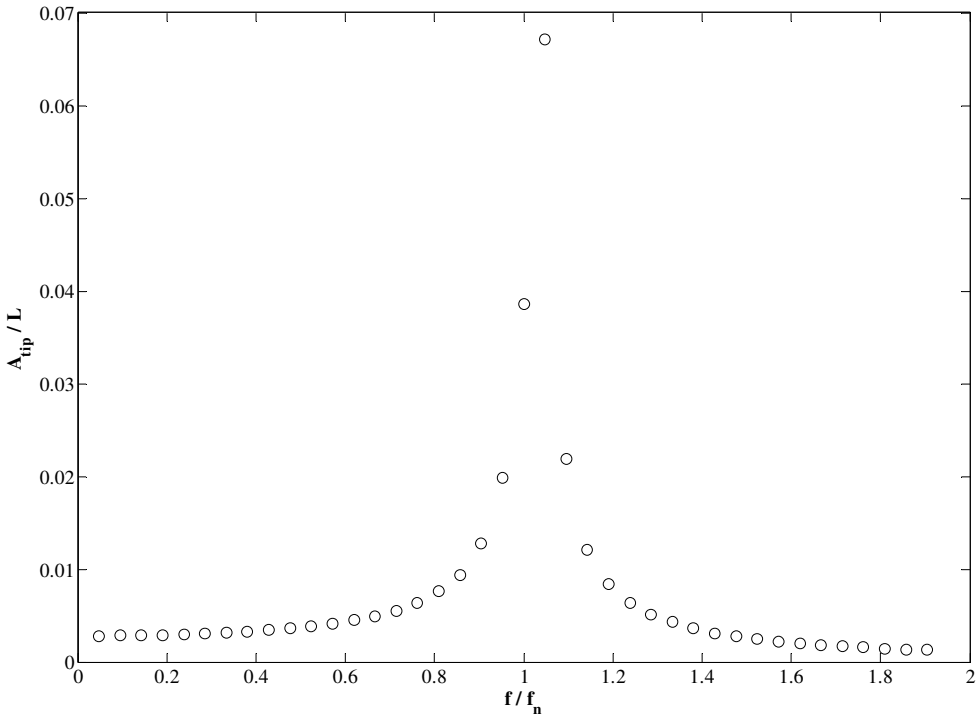

Figure 18: Nonlinear model with a maximum velocity of 5 m/s for a branch with variable EI and diameter.

CHAPTER 4

CONCLUSIONS

Previous studies on wind-induced oscillations have always involved in modeling the tree as a linear structure. In this thesis, a nonlinear model for wind-induced oscillations of trees is derived. The structural nonlinearities are considered and it is shown that by considering such nonlinearities, hardening behavior is observed in the tree's response. Such behavior implies that for certain range of wind frequencies, trees can oscillate with either a small amplitude or a large amplitude. The small-amplitude oscillations can be predicted without taking into account the structural nonlinearities, but the large-amplitude oscillations are predicted only when the structural nonlinearities are considered. The influence of various system parameters (wind profile, tree's taper, slenderness ratio, etc.) are also considered, and it is shown that the hardening effect occurs over a wide range of system parameters. This means that the hardening effect is natural to the system and is not the result of using a unique set of parameters.

The model is not completely realistic. The addition of crown as a lumped mass and the porosity of the crown have to be taken into account. Crown asymmetry also plays a part in affecting the wind-induced oscillations. A much more complete 3D model of the tree can be derived, taking the transverse oscillations into account.

BIBLIOGRAPHY

[1] Allen J.R.L. 1992. Trees and their response to wind: Mid Flandrian Strong winds, Severn Estuary and Inner Bristol Channel, Southwest Britain. Philosophical Transactions: Biological Sciences London 338:335-64.

[2] Deresse T. 1998. Wood properties of Red Pine. Maine Agricultural and Forest Experimentation Station Miscellaneous Report 412:1-16.

[3] Ennos A.R. 1999.The aerodynamics and hydrodynamics of plants. Journal of Experimental Biology 202:3281-84.

[4] Gardiner B.A. 1992. Mathematical modeling of the static and dynamic characteristics of plantation trees. Mathematical modeling of forest ecosystems: proceedings of a workshop organized by Fortsliche Versuchsanstalt Rheinland-Pfalz and Zentrum für Prakt:40-61.

[5] Gardiner B.A. and Quine C.P. 2000. Management of forests to reduce the risk of abiotic damage – a review with particular reference to the effects of strong winds. Forest Ecology and Management 135:261-77.

[6] Haritos N. and James K. 2008. Dynamic response characteristics of trees from excitation by turbulent wind. 20th Australasian conference on the Mechanics of Structures and Materials: 147-52.

[7] James K. 2003. Dynamic loading of trees. Journal of Arboriculture 29(3):165-71.

[8] Kane B. and Smiley T.E. 2006. Drag coefficients and crown area estimation of red maple. Canadian Journal of Forest Research 36:1951-58.

[9] Kane B. and Smiley T.E. 2006. The effects of pruning type on wind loading of *Acer Rubrum*. Arboriculture and Urban Forestry 32(1):33-39.

[10] Kane B., Pavlis M., Harris R.J. and Seiler J.R. 2008. Crown reconfiguration and trunk stress in deciduous trees. Canadian Journal of Forest Research 38:1275-89.

[11] Kerzenmacher T. and Gardiner B.A. 1998. A mathematical model to describe the dynamic response of a spruce tree to the wind. Trees 12:385-94.

[12] Kim Y.M. and You K.P. 2002. Dynamic responses of a tapered tall building to wind loads. Journal of Wind Engineering and Industrial Aerodynamics 90:1771-82.

[13] Mayhead G.J. 1973. Some drag coefficients for British forest trees derived from wind tunnel studies. Agricultural Meteorology 12:123-30.

[14] Mortimer M.J. and Kane B. 2004. Hazard tree liability in the United States: uncertain risks for owners and professionals. Urban Forestry and Urban Greening 2(3):159-65.

[15] Moulia B, Combes D. 2006. Thigmomorphogenetic acclimation of plants to moderate winds as a major factor controlling height growth and biomass distribution in crops, as demonstrated in alfalfa (*Medicago sativa* l.). Proceedings of Plant Biomechanics conference Stockholm:STFI:317-22.

[16] Papesch A.F.G. 1974. A simplified theoretical analysis of the factors that influence windthrow of trees. 5th Australasian conference on Hydraulics and Fluid Mechanics:235-42.

[17] Peltola H., Kellomäki S., Väisänen H. and Ikonen V.-P. 1999. A mechanistic model for assessing the risk of snow and wind damage to single trees and stands of Scots pine, Norway spruce and birch. Canadian Journal of Forest Research 29:647-661.

[18] Ray M.L., Rogers A.L. and McGowan J.G. 2006. An investigation of wind shear models and experimental data trends for different terrains. Wind Engineering 30: 341-50.

[19] Roden J. 2003. Modeling the light interception and carbon gain of individual fluttering aspen (*Populus tremuloides* Michx)leaves. Trees Structure and Function 17:117-26.

[20] Saunderson S.E.T., England A.H. and Baker C.J. 1999. A dynamic model of the behaviour of Sitka spruce in high winds. Journal of Theoretical Biology 200:249-59.

[21] Semler C., Gentleman W.C. and Paidoussis M.P. 2006. Numerical solutions of second order implicit non-linear ordinary differential equations. Journal of Sound and Vibration 195(4):553-74.

[22] Spatz H. and Bruechert F. 2000. Basic biomechanics of self-supporting plants: wind loads and gravitational loads on a Norway spruce tree. Forest Ecology and Management 135:33-44.

[23] Spatz H., Bruechert F. and Pfisterer J. 2007. Multiple resonance damping or how do trees escape dangerously large oscillations. American Journal of Botany 94(10):1603-11.

[24] Stokes V, Morecroft M, Morison J. 2006. Boundary layer conductance for contrasting leaf shapes in a deciduous broadleaved forest canopy. Agricultural and forest meteorology 139:40-54.